JOURNAL OF NEUROTRAUMA 36:2977–2990 (November 1, 2019)
Mary Ann Liebert, Inc.
DOI: 10.1089/neu.2018.6332

Neuroectodermal Stem Cells Grafted into the Injured Spinal Cord Induce Both Axonal Regeneration and Morphological Restoration via Multiple Mechanisms

Krisztián Pajer,[1] Tamás Bellák,[1] Heinz Redl,[2] and Antal Nógrádi[1,2]

Abstract

Spinal cord contusion injury leads to severe loss of gray and white matter and subsequent deficit of motor and sensory functions below the lesion. In this study, we investigated whether application of murine clonal embryonic neuroectodermal stem cells can prevent the spinal cord secondary damage and induce functional recovery. Stem cells (NE-GFP-4C cell line) were grafted intraspinally or intravenously immediately or one week after thoracic spinal cord contusion injury. Control animals received cell culture medium or fibrin intraspinally one week after injury. Functional tests (Basso, Beattie, Bresnahan, CatWalk®) and detailed morphological analysis were performed to evaluate the effects of grafted cells. Stem cells applied either locally or intravenously induced significantly improved functional recovery compared with their controls. Morphologically, stem cell grafting prevented the formation of secondary injury and promoted sparing of the gray and white matters. The transplanted cells integrated into the host tissue and differentiated into neurons, astrocytes, and oligodendrocytes. In intraspinally grafted animals, the corticospinal tract axons regenerated along the ventral border of the cavity and have grown several millimeters, even beyond the caudal end of the lesion. The extent of regeneration and functional improvement was inversely related to the amounts of chondroitin sulphate and ephrin-B2 molecules around the cavity and to the microglial and astrocytic reactions in the injured segment early after injury. The grafts produced glial cell derived neurotrophic factor, macrophage inflammatory protein-1a, interleukin (IL)-6 and IL-10 in a paracrine fashion for at least one week. Treating the grafted cords with neutralizing antibodies against these four factors through the use of osmotic pumps nearly completely abolished the effect of the graft. The non-significant functional improvement after function blocking is likely because the stem cell derivatives settled in the injured cord. These data suggest that grafted neuroectodermal stem cells are able to prevent the secondary spinal cord damage and induce significant regeneration via multiple mechanisms.

Keywords: functional recovery; paracrine mechanism; regeneration; spinal cord injury; stem cells

Introduction

Spinal cord injury (SCI) results in irreversible tissue damage accompanied by motor, sensory, and vegetative function losses and is followed by very limited recovery of function.[1,2] Although the physical damage caused by the injury cannot be overcome, secondary injuries can be prevented partially.[3–8] In addition to this, recently serious efforts have been made to render the microenvironment of the lesion permissive to growing axons, thus promoting regeneration within the damaged cord. Therapeutic strategies aiming at fostering regeneration included the down-regulation of several axonal growth-inhibiting factors such as ephrins and their receptors,[9–12] myelin-derived inhibitors,[13–15] and the chondroitin-sulphate family.[16,17]

In the last decades, intensive efforts to restore the lost integrity of the injured spinal cord included the use of various neuroprotective substances, such as riluzole and cell-based therapeutic approaches. Some of the stem cell-based therapeutic applications were able to induce both morphological and functional neuroprotection ands in some cases regeneration.[18–23]

Earlier studies from our laboratory have provided evidence that the immortalized neuroectodermal stem cell line NE-GFP-4C

[1]Department of Anatomy, Histology, and Embryology, Faculty of Medicine, University of Szeged, Szeged, Hungary.
[2]Ludwig Boltzmann Institute for Experimental and Clinical Traumatology, Vienna, Austria.

(ATCC No.: CRL-2936), derived from the forebrain vesicle wall of p53-deficient nine-day–old mouse embryos[24] effectively prevents the death of motoneurons destined to die after a spinal ventral root avulsion injury. The NE-GFP-4C cells have been shown to differentiate to neurons, astrocytes, and oligodendrocytes after transplantation into the spinal cord with a damaged motoneuron pool and induced the rescue of the vast majority of the injured motoneurons.[25,26] It has been proven that the grafted cells' secretome induced by the motoneuron damage was able to support motoneuron survival.[26]

Based on the capacity of NE-GFP-4C cells being able to rescue severely injured motoneurons and promote the regeneration of their axons, we hypothesized that transplantation of these cells into a contused spinal cord may lead to robust morphological regeneration and restoration of function after injury. The aim of the present study was to investigate the changes in the microenvironment of the injured cord after transplantation of NE-GFP-4C cells.

Methods

Maintenance of NE-GFP-4C stem cells

The NE-GFP-4C clonal neuroectodermal stem cells (ATCC No. CRL-2926) were isolated from forebrain vesicles of nine-day–old embryos of transgenic mice lacking the tumor suppressor gene p53, and they were made to produce eGFP as described previously.[24] The NE-GFP-4C cells were maintained on Nunc™ Petri dishes (Invitrogen, Austria) in High glucose Dulbecco Modified Essential Medium (H-DMEM, Sigma, Austria) supplemented with 10% fetal calf serum (FCS, Gibco, ThermoFischer Scientific, Waltham, MA) at 37°C and 5% CO_2.

SCI model

All together, 90 female Sprague-Dawley rats (Animal Research Laboratories, Himberg, Austria, 180–220 g body weight) were used. All of the operations were performed under deep ketamine-xylazine anesthesia (ketamine hydrochloride [Ketavet, 110 mg/kg body weight]; xylazine [Rompun, 12 mg/kg body weight]) and sterile precautions. Laminectomy was performed at the thoracic 11 (T11) vertebral level, the dura mater was exposed, and the spinal cord was contused using an Infinity Horizon impactor (IH-0400, PSI LLC, Glendale, CA), applying 150 kdyn force. All animals were allowed to survive two, three, or eight weeks after injury.

The experiments were performed with the approval of the Animal Protocol Review Board of City Government of Vienna regarding the care and use of animals for experimental procedures. All the procedures were performed according to the Helsinki Declaration on Animal Rights. Animals were given food and water *ad libitum.*

Transplantation of NE-GFP-4C stem cells and experimental groups

Immediately or one week after injury, NE-GFP-4C cells were transplanted intravenously or intraspinally (depending on the experimental setup) using Hamilton pipettes. Intravenously 1×10^6 (delivered in 250 microliter medium), intraspinally 5×10^5 stem cells (delivered in 2 microliter) were injected into the tail vein or into the lesion cavity, respectively. In the case of intraspinal application, a one week delay of the transplantation was applied based on the study by Péron and associates.[27] This study has shown that such delay of the transplantation significantly enhances the survival and proliferation of the grafted cells.[27]

In a separate experimental group, stem cells were grafted intraspinally mixed with human fibrin clot matrix (Baxter Healthcare Corporation, Westlake Village, CA, 500 IU/mL, human). Control animals received medium or fibrin intraspinally or medium intravenously one week or medium intravenously immediately after injury.

The following experimental groups (n = 10) were established in this study:

1. Fibrin-1w-isp: fibrin was injected intraspinally one week after injury (control).
2. Medium-1w-isp: medium was injected intraspinally one week after injury (control).
3. Medium-immed-iv: medium was injected intravenously immediately after injury (control).
4. Medium-1w-iv: medium was injected intravenously one week after injury (control).
5. NE4C-fibrin: stem cells in fibrin were transplanted intraspinally one week after injury.
6. NE4C-immed-iv: stem cells were transplanted intravenously immediately after injury.
7. NE4C-1w-iv: stem cells were transplanted intravenously one week after injury.
8. NE4C-1w-isp: stem cells were transplanted intraspinally one week after injury.

Further, two groups ($n = 5$) were set up in separate experiments using function blocking antibodies; for details, see below.

9. NE4C-isp-blocking: function blocking antibodies were used intraspinally after one week of injury.
10. NE4C-isp-isospecific: isospecific antibodies were used intraspinally after one week of injury (control).

Retrograde labeling

Eight weeks after surgery, five animals with long-term survival (groups 1, 2, 5, 6, 7, 8) were deeply anesthetized as described above. The L3 spinal segment was exposed, and a right hemisection was performed. Fast Blue (FB) crystals (Illing Plastics GmbH, Gross-Umfeld, Germany) were placed into the gap, and the wound was closed. Seven days after the application, the animals were reanesthetized and perfused transcardially. Sections taken from the brain and spinal cord were cut in a cryostat (Leica CM-1850, Leica GmbH, Germany) and mounted onto gelatinized slides. The number of FB-positive cells was determined using an epifluorescent microscope (BX-50, Olympus, Japan).

Anterograde labeling

In the long-term survival groups (8 weeks survival, groups 1, 2, 5, 6, 7, and 8, $n = 5$ animals in each group), the rats were anesthetized, and the left hind limb area of the motor cortex was microinjected stereotaxically with 4×2 μL of biotinylated dextran-amine (BDA, MW 10000; Molecular Probes) in phosphate buffered saline (PBS).[28] One week after the BDA administration, animals were reanesthetized and perfused transcardially. After cryosectioning, the BDA-labeled fibers were visualized by using the Tyramide Alexa protocol. For camera lucida drawings, three parasagittal sections were used and the camera lucida drawings were superimposed on each other.

Sacrifice of animals and maintenance of samples

After various survival times (2, 3, or 8 weeks after injury), animals were anesthetized and perfused transcardially with saline containing heparin followed by 4% paraformaldehyde (PFA) in 0.1 mol/L phosphate buffer (pH 7.4). The spinal cord, brainstem, and the brain of the animals were removed and placed into 4% buffered PFA for one day. The fixed tissues were cryoprotected in 30% sucrose in PBS containing 0.01% sodium-azide at 4°C until

being embedded in Shandon Cryomatrix gel (ThermoFischer Scientific, United Kingdom). Parallel or serial transverse (25 μm thick) and longitudinal (16 μm thick) sections were cut and mounted onto gelatine-coated glass slides.

Immuno- and lectin histochemistry

Non-specific binding sites were blocked subsequently with 3% normal donkey, goat, or horse serum. Primary antibodies and lectin were used as follows: rat anti-M6 (mouse-specific neuron marker, DSHB, 1:400), rat anti-M2 (mouse-specific astrocyte marker, DSHB, 1:400), rat anti-MOG (mouse-specific oligodendrocyte marker, R&D Systems, 1:50, MAB2439), rabbit anti-glial fibrillary acidic protein (GFAP) (Life Technologies, 1:400, 18-0063), chicken anti-beta(III)-tubulin (Merck-Millipore, 1:1000, ab9354), rabbit anti-beta(III)-tubulin (1:1000, Abcam, ab18207), rabbit anti-neurofilament 200kD (1:500, Abcam, ab8135), chicken anti-green fluorescent protein (GFP) (Merck-Millipore, 1:1000, ab16901), mouse anti-CS-56 (1:200, SIGMA, C8035), rabbit anti-Eph-A4 (1:500, Santa Cruz Biotechnology, sc-20721), goat anti-ephrin-B2 (1:500, Santa Cruz Biotechnology, sc-19227), biotinylated GriffoniaSimplicifoliaisolectin B4 (1:200, Vector, B1205), rabbit anti-IL-1-alpha (1:200, Abbiotech, 250715), goat anti-IL-6 (1:200, R&D Systems, AF-406-NA), rat anti-IL-10 (1:200, BioLegend, 505011), rabbit anti-tumor necrosis factor (TNF)-alpha (1:200, Abbiotech, 250844), goat anti-macrophage inflammatory protein (MIP)-1-alpha (1:200, R&D Systems, AF-450-NA), rabbit anti-NT-4/5 (1:200, Abbiotech, 250792), rabbit anti-brain-derived neurotrophic factor (BDNF) (1:200, Abcam, ab72439), rabbit anti-glial cell derived neurotrophic factor (GDNF) (1:200, Abcam, ab18956), rabbit anti-vascular endothelial growth factor (VEGF) (1:200, Santa Cruz Biotechnology, sc-507), rabbit anti-platelet-derived growth factor (PDGF)-A (1:200, Santa Cruz Biotechnology, sc-7958), rabbit anti-5-hydroxytryptamine (HT) (1:100, Abcam, ab10385) and goat anti-matrix metalloproteinase (MMP)-2 (1:200, Santa Cruz Biotechnology, sc-6838).

The following secondary antibodies were used: biotinylated horse anti-goat immune globulin G (IgG) (H+L, BA9500), biotinylated goat anti-rabbit IgG (H+L, BA1000), biotinylated horse anti-mouse IgG (H+L, BA2001), biotinylated goat anti-chicken IgG (H+L, BA9010) (1:200, all from VECTOR). The immune reaction was completed by using Alexa Fluor 546 donkey anti-goat (1:400, Thermo Fischer Scientific, A11056), Alexa Fluor 546 goat anti-rabbit IgG (1:400, Thermo Fischer Scientific, A11010), Alexa Fluor 594 donkey anti-rat IgG (1:400, Thermo Fischer Scientific, A-21209), Streptavidin Alexa Fluor 546 Conjugate (1:400, Thermo Fischer Scientific, S-11225), Streptavidin Alexa Fluor 405 Conjugate (1:400, Thermo Fischer Scientific, S-32351), or the Alexa Fluor 546 TSA kit (1:800, Tyramide Signal Amplification; Thermo Fischer Scientific, T20933).

Fluorescent images were obtained by using an epifluorescent microscope (BX-50, Olympus, Japan) or a compact confocal microscope (FluoView® FV10i, Olympus, Japan).

Quantitative assessment of anterograde and retrograde tracing

For quantifying anterograde labeled corticospinal axons, analysis was performed according to Hill and colleagues.[28] The BDA-labeled corticospinal axons were examined in every fourth paramedian section (16 μm thick) of the injured spinal cord. The labeled axons were visualized through the use of streptavidin Alexa Fluor 546 (1:400, Thermo Fischer Scientific, S-11225). A zero point was determined as the rostralmost part of the cavity. Fifteen lines, perpendicular to the rostrocaudal axis, were drawn 0.5 mm apart from 2 mm rostral to 5 mm caudal from the zero point; axons that crossed these lines were counted at 40 $\times$ magnification.

To normalize the number of BDA labeled corticospinal axons in various groups, the total number of fibers was quantified 7 mm rostral to the cranial end of the lesion cavity, and the percentage of total axons crossing the designated lines caudal to this point was determined.

The number of retrograde labeled neurons was determined according to Bunge.[29] Serial transverse sections (30 μm thick) were taken from the T5, T2, C6, and C2 spinal segments, and every fifth or every tenth coronal section (30 μm thick) was used from the brainstem or from the cerebral cortex, respectively. In the spinal cord serial sections, the FB-labeled neurons were mapped, and their location was compared with that of the labeled neurons in the neighboring sections. Thus, double counting of the same neuron was avoided.[19] In the case of brainstem and cortex sections, the number of FB-labeled neurons was determined in each section, and the final numbers were multiplied by five or 10, respectively.

Quantification of cavity length, cystic area, and tissue sparing

Every second transverse section from the T7–L1 segments containing the lesion cavity was stained with cresyl violet. The border between the intact tissue and the lesion cavity composed of small cysts was defined. Cavity length was determined by using the following equation: cavity length (mm) = section thickness (μm) $\times$ number of sections.

The whole cystic cross sectional area (lesion cavity area) at the level of the epicenter was determined as follows: the number of pixels of the reference area (1 mm^2) and that of the cystic area was computed through the use of the NIH ImageJ analysis software (imagej.nih.gov/ij). The pixel number of the cystic area was divided by that of the reference area, and the result was expressed in mm^2.

The percentage of spared white and gray matter was determined in a similar manner. Briefly, the number of pixels of the spared white and gray matter was measured at the epicenter (0) and 0.3, 0.6, 0.9, and 1.2 mm rostrally and caudally from it. Identical spinal cord segments of intact animals were used as reference values. The amount of spared white and gray matter in the lesioned animals was given as percentage of intact spinal cord values.

Quantification of 5-HT density

For quantifying serotonergic fibers, analysis was performed according to Karimi-Abdolrezaee and coworkers.[30] To assess 5-HT immunoreactivity, photographs were taken from cross sections of L2 ventral horns. The relative density of 5-HT immunoreactivity was measured in the animals of the medium-1w-isp, NE4C-immed-iv, NE4C-1w-iv, and NE4C-1w-isp groups ($n = 4$ in each). To determine the final density, the background of unstained samples as reference intensity was subtracted from the intensity of immunoreactive samples. The density was then normalized to the uninjured value.

Quantification of ephrin-B2, Eph-A4, GFAP, GSA-B4, and CS56 reactions two and three weeks after injury

To assess the density of ephrin-B2+, Eph-A4+, GFAP+, GSA-B_4+, and CS-56+ reactivities in spinal cords of injured and treated animals ($n = 4$ in each group), two sagittal sections (150 μm apart) containing the lesion cavity were analyzed for each marker. Microphotographs were taken, and the whole spinal cord section area including the cavity and a 2 mm long extension of the tissue rostrally and caudally from the cavity ends was analyzed. After measuring the relative densities (ImageJ, National Institutes of Health), the values of transplanted spinal cords were divided by the relevant densities of the injured cords (control animals) and

multiplied by 100. The background intensity of unstained samples was individually subtracted from the intensity of treated sections.

Quantification of host-derived GDNF, IL-6, IL-10, and MIP-1 alpha

To quantify the density of immunoreactivity of the four secretome factors in spinal cords of medium-1w-isp and NE4C-1w-isp animals ($n=4$ animals in each group), two sagittal sections (150 μm apart) excluding the lesion or grafted area were analyzed for each marker. Using the Image J software, we measured the relative density of immunochemical fluorescence signal of four factors along a 2 mm long extension of the tissue rostrally and caudally from the cavity ends or grafted area taking the total width of the cord. Then, the GDNF, IL-6, IL-10, and MIP-1 alpha intensities were divided by the outlined area to calculate the mean net intensity/unit area. We determined the level of background/autofluorescence by imaging unstained samples. This reference intensity was then subtracted from the average intensity to determine the net final density.

Function-blocking antibody experiments

Animals ($n=5$ in each set of experiments) were anaesthetized deeply, and contusion injury was performed as described above. One week after the contusion injury, the animals were grafted as described above, and a miniosmotic pump (Alzet Osmotic Pumps, Cupertino, CA; type 1002, 100 μL volume, actively pumping for 2 weeks) filled with a mixture of function-blocking antibodies against GDNF (AF-212-NA), IL-6 (AF-406-NA), MIP-1a (AF-450-NA) (4 μg/mL working concentration, all from R&D Systems, Minneapolis, MN), and IL-10 (Biolegend, San Diego, CA, 505011) was placed subcutaneously in the dorsal region (group 9., NE4C-intraspin-blocking). All antibodies were specific to mouse epitopes only.

A silicone tube (Degania Silicone Ltd, Kibbutz Degania, Israel, 0.3 mm in internal diameter) extended from the minipump to the spinal cord, and its distal end was inserted into the dorsal part of the cord at the site of grafting into the contusion cavity. The tube was fixed to the surrounding musculature with 8-0 sutures (Ethilon) to avoid moving in or out of the spinal cord.

Control animals received NE-GFP-4C stem cell grafts and pumps filled with identical volumes of antibody-specific IgG isotypes only including polyclonal goat IgG for the replacement of GDNF, IL-6, MIP-1-alpha antibodies, and monoclonal rat IgG2A for the replacement of IL-10 antibody (4 μg/mL working concentration, all from R&D Systems, Minneapolis, MN) (group 10, *NE4C-intraspin-isospecific*). Motor function was evaluated weekly for eight weeks by applying the Basso, Beattie, Bresnahan (BBB) test.[31] After eight weeks survival time, rats were processed for histological analysis.

Analysis of locomotion pattern—CatWalk® gait analysis

To determine and analyze the parameters of the movement pattern, the CatWalk automated quantitative gait analysis system[32] (Noldus Ltd, The Netherlands) was used ($n=8$ each in groups 1–8, except group 5 where the analysis could not be performed). The following parameters were taken into account during the analysis: max area, print area, stride length, swing duration, and swing speed. We measured these parameters eight weeks after the injury. Animals had a two-week–long training period before the contusion injury. Data were evaluated by the CatWalk software.[32,33]

Open field test

In the long-term survival groups (8 weeks), motor function was evaluated by the BBB test[31] three days after the injury and then once a week for eight weeks. Two observers, unaware of experimental procedures, tested the animals ($n=8$ in each group, except groups 9 and 10 where $n=4$).

Statistical analysis

The paired *t* test or the one-way analysis of variance (ANOVA) or the two-way ANOVA test followed by the Tukey all pairwise multiple comparison procedure were used to compare the data.

Results

General observations, functional improvement, and CatWalk gait analysis

The BBB open field test was used at regular intervals to assess locomotor recovery. After the contusion injury, all animals displayed strong motor impairment. During the first week, no weight supported stepping was observed in all groups (Fig. 1A). Intraspinal application of stem cells (NE4C-1w-isp) or medium (medium-1w-isp) on week 1 after the injury induced a plateau in locomotor recovery for one week. This phenomenon is because of the minimally invasive nature of intraspinal grafting of cells or injection of medium. In contrast, systemic application of stem cells (NE4C-immed-iv, NE4C-1w-iv) or medium (medium-1w-iv) did not induce any drop in locomotor recovery (Fig. 1A).

Four weeks after the injury, the animals that received intraspinal grafts displayed the same BBB scores as the intravenously grafted groups. From five to eight weeks after injury, consistent plantar stepping with predominant parallel paw position and consistent fore- and hindlimb coordination could be observed in the animals that received systemic and intraspinal grafts. Interestingly, animals whose spinal cord cavity was filled with NE-GFP-4C cells mixed with fibrin (NE4C-fibrin) had more impaired locomotion than their controls (fibrin-1w-isp; Fig. 1A,B). These animals showed occasional weight supported dorsal or plantar stepping without fore- and hindlimb coordination.

The results of the automated gait analysis (CatWalk) confirmed our functional observations on freely moving animals (Fig. 1C). We evaluated the print and maximum area of hindlimb, swing duration, swing speed, and stride length eight weeks after injury. The animals of the NE4C-fibrin group could not be processed for CatWalk analysis because these rats displayed only occasional weight support. The functional recovery was significantly improved in the intravenously and intraspinally grafted groups (NE4C-immed-iv, NE4C-1w-iv, and NE4C-1w-isp) compared with their controls.

Stem cells induce tissue sparing

Within the injured segment, a large, centrally located cystic cavity was formed containing cellular debris. The morphological analysis involved measuring the rostrocaudal distribution of spared gray and white matter in the injured segments eight weeks after the injury. Both the intravenous and intraspinal application of stem cells resulted in significantly improved tissue sparing relative to the controls. The highest percentage of spared tissue was detected in those animals that received intraspinal grafts (NE4C-1w-isp) (Supplementary Fig. S1A; see online supplementary material at www.liebertpub.com). The intravenously treated animals (NE4C-immed-iv and NE4C-1w-iv) also displayed high, but non-significantly lower amount of spared tissue compared with the intraspinally treated animals (Fig. S1A). The greatest amount of white matter localized to the ventral and ventrolateral parts of the spinal cord in

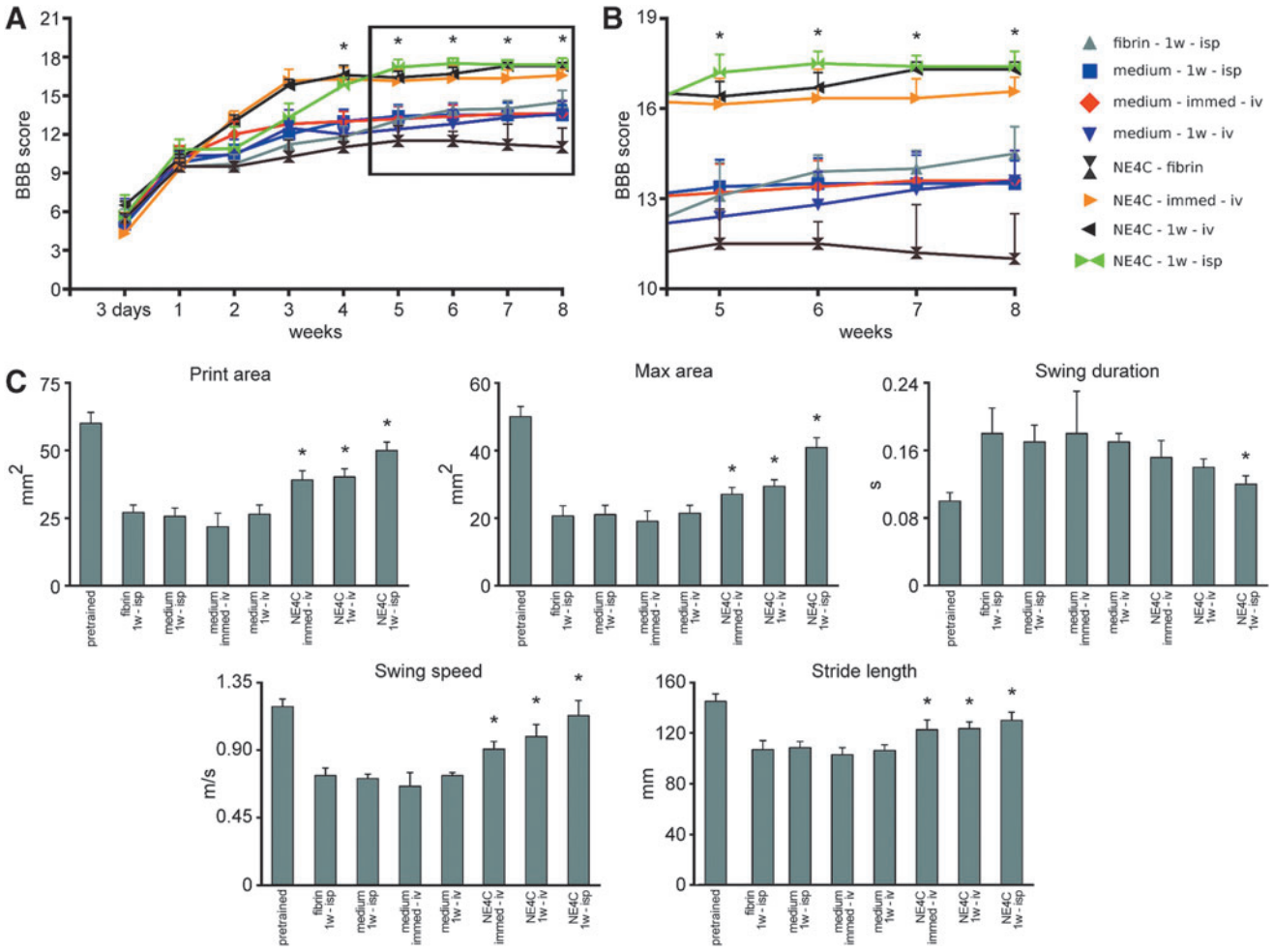

FIG. 1. Locomotor analysis of the grafted animals and their controls. (**A**) Open field locomotor test (Basso, Beattie, Bresnahan [BBB]) shows significant improvement in all grafted animals compared with their controls, except the NE4C-fibrin one, which showed a decline of their locomotor pattern from week 6 onward. (**B**) Enlarged view of the graphs in A from week 5 onward. Note the grouping of locomotor scores in the grafted and control groups except for the NE4C-fibrin animals. Asterisk represents significant difference between each grafted group and its control at various time points (with exception of the NE4C-fibrin group). (**C**) Semiautomated CatWalk® gait analysis of the animals in the various groups eight weeks after injury. Note the significantly improved parameters of the grafted animals compared with their controls. The NE4C-fibrin animals could not be evaluated in the CatWalk locomotor analysis system because in many instances they did not produce well-recordable runs. Data are expressed as mean ± standard error of the mean. *, significant difference between the intraspinally or intravenously grafted animals with the control ones. Color image is available online.

these groups. In contrast, in animals treated with stem cells mixed with fibrin (NE4C-fibrin), the spared white and gray matter was smaller than in all the other groups (Fig. S1A).

The basic parameters of the cavity such as lesion area at the epicenter and length of the cavity on week eight after the injury revealed that both the intravenously and intraspinally treated animals (NE4C-immed-iv, NE4C-1w-iv, NE4C-1w-isp) had significantly smaller cavity length and lesion area than their controls. No significant difference was found in animals that received their stem cells embedded in fibrin (NE4C-*fibrin)* compared with their control group (Supplementary Fig. S1B,C; see online supplementary material at www.liebertpub.com).

Retrograde neuronal tracing analysis

Next, we evaluated whether axonal regeneration/sparing was promoted by the grafted stem cells. Retrograde labeling with the fluorescent dye FB from the right L3 segment revealed that significantly higher numbers of FB-labeled propriospinal neurons were found in the T5, T2, C6, and C2 spinal segments in animals treated with stem cells (NE4C-immed-iv, NE4C-1w-iv, and NE4C-1w-isp) than in their controls. The number of retrogradely labeled neurons in the NE4C-fibrin group was not statistically different from the control groups (Fig. 2A).

Both the total number of FB cells in the brainstem and their number in the selected brainstem nuclei (reticular formation, lateral vestibular nucleus, and inferior olivary nucleus) projecting distally to the lesion site were significantly higher compared with their controls. This was also the case for layer V neurons in the motor cortex whose axons rarely were able to project into the distal spinal cord. Only the intraspinally grafted animals (NE4C-1w-isp) showed an exception because these rats displayed significantly greater numbers of retrograde labeled pyramidal cells compared with the controls and the intravenously grafted animals (NE4C-immed-iv, NE4C-1w-iv; Fig. 2A).

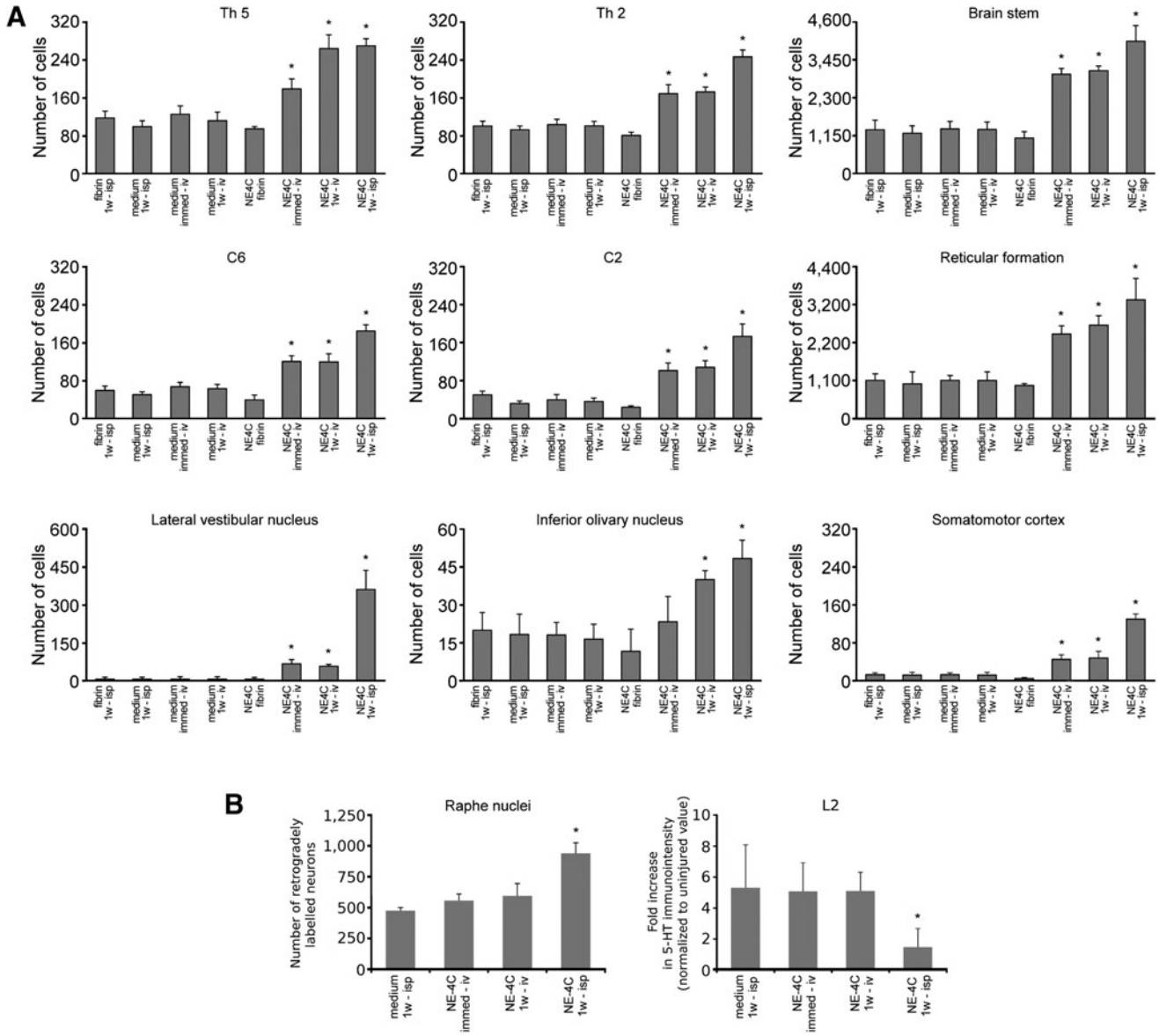

FIG. 2. Morphometric analysis of the connections between the segments caudal to the lesion and various parts of the central nervous system cranial to that. (**A**) Numbers of neurons retrograde labeled from the right L3 hemisegment. Note the significantly higher numbers of labeled cells in the grafted animals compared with their controls, especially in the brainstem. The greatest number of retrograde labeled cells was always found in the intraspinally treated animals. (**B**) Retrograde labeling results in the raphe nuclei (left panel) and serotonergic immunochemical densities (right panel) expressed as fold increase caudal to the lesion normalized to the uninjured level. Note the considerable number of retrograde labeled raphe neurons and the lack of sprouting in the NE4C-1w-isp animals. Data are expressed as mean ± standard error of the mean. *, significant difference between the intraspinally or intravenously grafted animals with the control ones.

In contrast, the raphe nuclei of animals that received intraspinal grafts (NE4C-1w-isp) displayed significantly more FB-labeled neurons than those of intravenously grafted animals (NE4C-immed-iv, NE4C-1w-iv) or their controls (Fig. 2B).

Preservation of serotonergic innervation after intraspinal grafting

Serotonergic fibers reportedly exert strong supraspinal influence on locomotion.[34–36] Sprouting of the remaining 5-HT+ fibers caudal to a contusion injury is found to be limited by successful therapeutic approaches.[30] Accordingly, descending serotonergic fiber density was measured caudal to the injury in the ventral horn of the L2 spinal segment of intravenously and intraspinally grafted animals (NE4C-immed-iv, NE4C-1w-iv, NE4C-1w-isp) and in the control group (medium-1w-isp). We found a 5-to-5.7–fold increase of 5-HT+ fiber density in the control and in the intravenously grafted groups. In contrast, a small, 1.8-fold increase of density was observed in the intraspinally grafted animals compared with the uninjured value (Fig. 2B).

Anterograde corticospinal tracing analysis

Our retrograde labeling studies have suggested that significantly greater numbers of corticospinal axons were spared or have regenerated in the intraspinally grafted animals. To distinguish

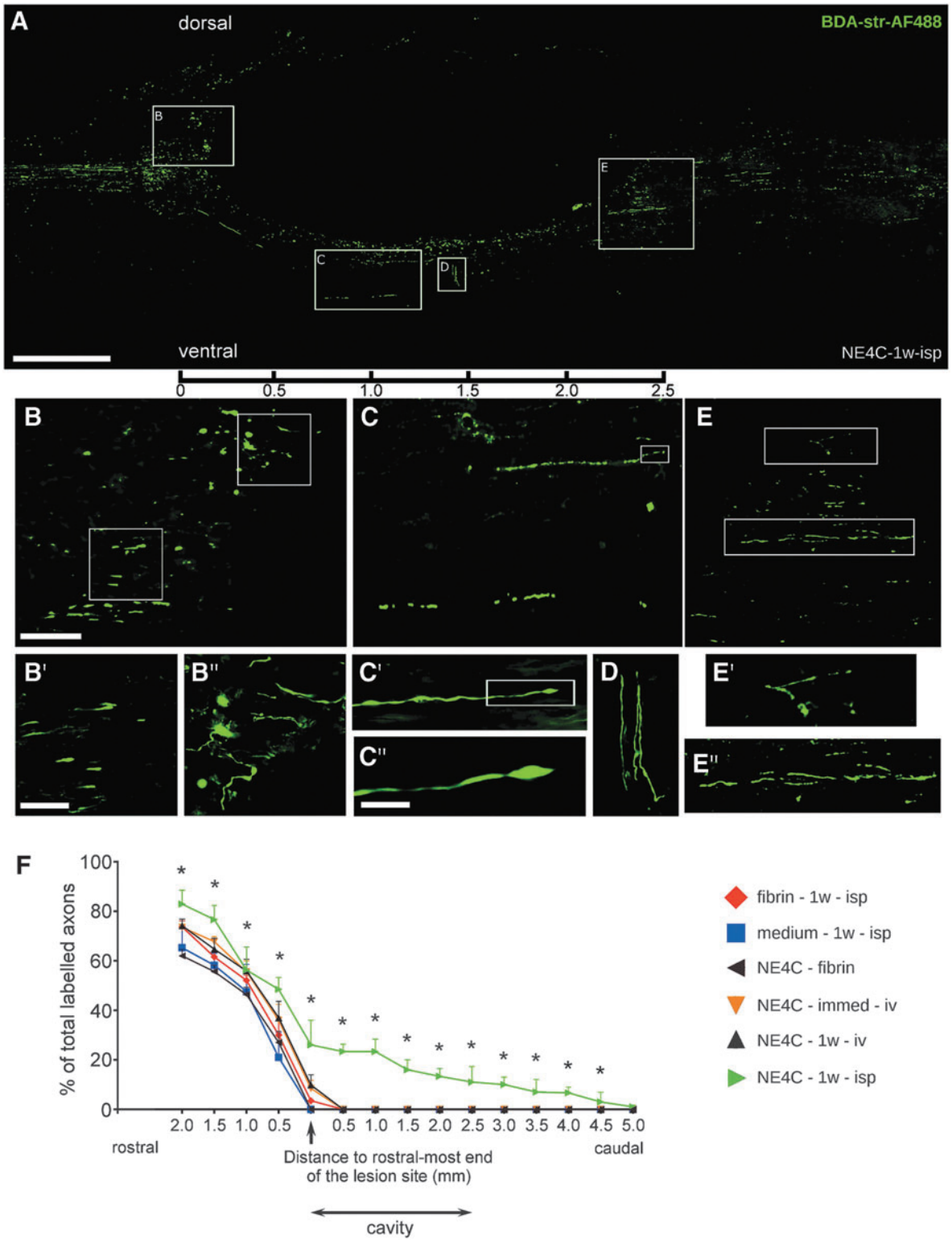

FIG. 3. Regeneration of corticospinal tract (CST) fibers in the spinal cords of NE4C-1w-isp animals. (**A**) Paramedian sagittal section of a representative NE4C-1w-isp spinal cord showing the biotinylated dextran-amine (BDA)–labeled CST fibers. The images of three neighboring sections are superimposed to show the significant numbers of regenerating axons. (**B**) Many dorsally growing fibers reach the cranial end of the cavity where they form axon growth cone-like structures and aborted, club-like endings (see enlarged framed area B in B′ and B″). (**C**) Considerable numbers of regenerating axons form a new pathway along the ventral edge of the cavity. Some of them still display growth cone-like structure at their tips eight weeks after injury (see boxed area C′ enlarged in C″). (**D**) Few axons get diverted at this level and grow perpendicular to the longitudinal axis of the cavity. (**E**) Regenerating axons re-enter the original pathway and then grow along the vacated fiber tract. Enlarged boxes E′ and E″ show the course of these fibers. Scale bars: A: 500 μm, B: 100 μm, B′: 50 μm, C″: 10 μm. (**F**) Graph shows the cumulative ratios of anterograde labeled CST fibers in the various experimental groups (100% corresponds to the total number of labeled CST fibers in the intact cranial part of the cord). Only animals in the NE4C-1w-isp group were able to regenerate their CST axons beyond the caudal end of the remaining contusion cavity. Data are expressed as mean ± standard error of the mean. *, significant difference between NE4C-1w-isp group with the control group (medium-1w-isp). Color image is available online.

between spared and regenerating corticospinal axons, we performed anterograde labeling of pyramidal cells in the motor cortex. The BDA-labeling of pyramidal cells in control animals displayed retracted corticospinal tract (CST) axons with bulb-like endings approaching 300 μm at the rostral end of the lesion cavity. In most of the treated animals, the CST axons were able to reach the rostral end of the cavity, but did not grow further along (Supplementary Fig. S2; see online supplementary material at www.liebertpub.com).

Most interestingly, CST axons in more than half of the intraspinally grafted animals (NE4C-1w-isp, three of five animals) showed profound regeneration. In these animals the CST axons regenerated all the way along the ventral border of the cavity of the cord, and a significant number of these regenerating fibers returned

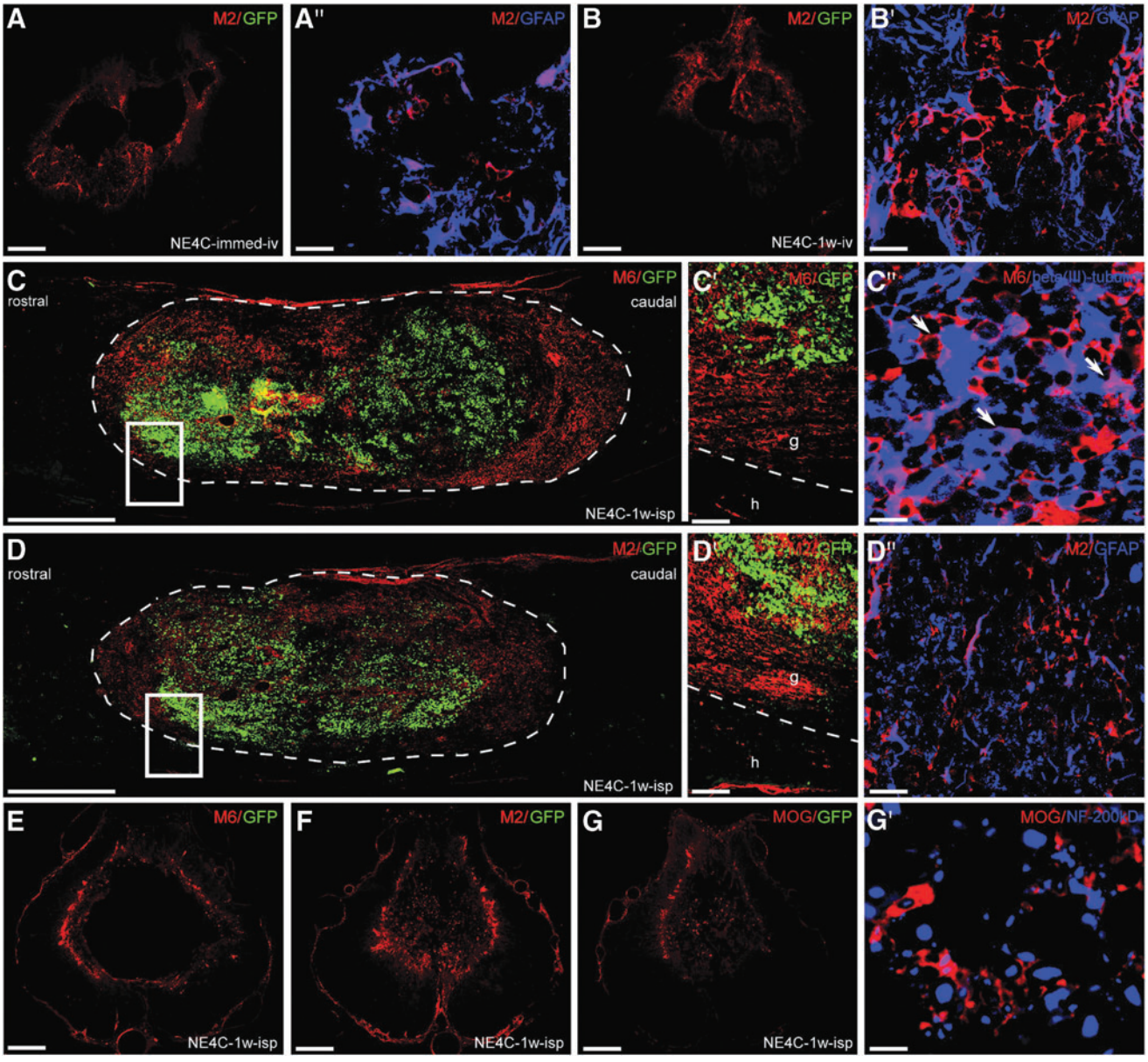

FIG. 4. Fate and differentiation of the grafted NE-GFP-4C cells are shown in the various grafting paradigms. (**A,B**) The derivatives of the intravenously grafted NE-GFP-4C cells (A-A′: NE4C-immed-iv, B-B′: NE4C-1w-iv) settled in the wall of the contusion cavity one week after grafting are displayed. Most of the M2-positive cells express glial fibrillary acidic protein (GFAP). A′ and B′ show randomly selected high magnification fields. (**C,D**) Differentiation of intraspinally grafted NE-GFP-4C cells in the contusion cavity one week after grafting results in the appearance of glial and neuronal derivatives at the periphery of the graft. Boxed areas are shown in C′-C″ and D′-D″. C′-C″: High numbers of M6 positive neuronal derivatives are expressing beta(III)-tubulin. D′-D″: M2 positive astroglial cells also co-express GFAP. (**E–G**) Intraspinally grafted stem cell derivatives remain in the wall of the cavity at the end of the survival period (eight weeks after grafting). Apart from the neuronal and glial stem cell-derived cells (**E,F**), mouse-specific oligodendrocyte marker (MOG) positive oligodendrocytes are also present in the wall of the cavity (**G**) and appeared to be in close relation to NF-200 positive axons (G′). Note that green fluorescent protein (eGFP) expression pattern diminishes with differentitation (A,B,C,D,E,F,G). Dashed line indicates the graft-host border. A,B: 250 μm, A′, B′: 20 μm, C,D: 500 μm, C′, D′: 20 μm, C″: 10 μm; D″: 20 μm, E F,G: 250 μm, G′: 10 μm. Color image is available online.

to their original CST pathway at levels caudally to the distal end of the cavity (Fig. 3A).

These far regenerating axons appeared to grow for distances of at least 5 mm taken from the rostral end of the cavity (Fig. 3F). Moreover, axon growth cone-like structures and aborted, club-like endings could be detected around the rostral end of the cavity (Fig. 3B, B′, B″) and along the regenerating ventral pathway (Fig. 3C, C′, C″, D). The BDA-labeled fibers were also found at the caudal end of the cavity (Fig. 3E, E′, E″). Significant difference was found in the axon numbers between intraspinally grafted (NE4C-1w-isp) and the control animals (medium-1w-isp) (Fig. 3F).

Differentiation of the grafted cells in the injured cord

To determine the differentiation potential of the grafted stem cells in the injured cord, we analyzed the expression of murine markers that are able to uniquely identify grafted mouse cells in a rat environment (Fig. 4). One week after intravenous transplantation (NE4C-immed-iv, NE4C-1w-iv), only M2-positive astrocytes could be seen in the injured cord, and all these cells disappeared by the end of the investigation period. Stem cell-derived astrocytes settled down mainly in the wall of the cavity and expressed the glial marker GFAP (Fig. 4A,A′,B,B′).

In contrast, the intraspinally grafted stem cells (NE4C-1w-isp) differentiated into neurons (M6+) and astrocytes (M2+) one week after transplantation (Fig. 4C,C′,D,D′). Stem cell-derived oligodendrocytes could not be detected at this stage. The majority of these stem cell-derived neurons and astrocytes also expressed beta(III)-tubulin and GFAP, respectively (Fig. 4C″,D″). The grafted cells filled the cystic cavity without migrating out of it to the surrounding spinal cord tissue. At the end of the survival period stem cell-derived neurons, astrocytes and oligodendrocytes (MOG+) were found in the wall of the cavity (Fig. 4E,F,G). Neurofilament 200kD+ and MOG+ profiles were observed in close relationship to each other indicating that the stem cell-derived oligodendrocytes might have contributed to the remyelination of naked axons (Fig. 4G′). The eGFP expression of the grafted cells had decreased or ceased, suggesting that the eGFP expression pattern diminishes with differentiation confirmed by our earlier study, too.[26]

Modulation of the lesion environment

Next, we investigated whether the grafted cells have the potential to alter the microenvironment of the lesion rendering it permissive for regenerating axons. Therefore, we examined the densities of astrocytes and microglia/macrophages, the expression of Eph-A4 and ehprin-B2 molecules, and the deposition of chondroitin sulfate proteoglycan (CSPG) two and three weeks after the injury around the lesion cavity (Supplementary Fig. S3A,B; see online supplementary material at www.liebertpub.com). Both intraspinal or intravenous applications of stem cells induced significant reduction of astrocytosis at both time points indicated by significantly lower GFAP densities in these cords compared with their controls. Decreased GFAP densities were accompanied in these animals by limited CS-56+ depositions (Supplementary Fig. S3A,B).

Strong astrocytic reaction, however, was detected in animals that received stem cells in fibrin glue (NE4C-fibrin). Accordingly, CS-56 densities in these animals were as high as in their controls. Moreover, microglia/macrophage densities paralleled that of the astrocytes indicating a close link between the proliferation of these cell types.

Earlier studies have shown that after SCI, EphA receptor subtypes and their ephrin ligands are upregulated, and these interactions may create an environment that is unfavorable for neurite outgrowth and functional regeneration.[9,37,38] The EphA4-ephrinB2 binding reportedly induces collapse of neural growth cones in the presence of reactive astrocytes.[10,39,40] While EphA4 expression did not change significantly in the systemic and intraspinal treatment groups, ephrinB2 expression was found significantly lower in the intraspinally grafted animals two and three weeks after injury. The same effect was noted in the systemic treatment group only on week three (Supplementary Fig. S3A,B; see online supplementary material at www.liebertpub.com).

Increased MMP-2 expression in the graft two weeks after injury

The MMPs are thought to regulate the composition and permissiveness of the extracellular matrix.[41] Within this family, MMP-2 has been reported to prevent the development of massive glial scar tissue after central nervous system (CNS) injury.[42–44] Accordingly, expression of MMP-2 both in the host cord and the graft was analyzed two weeks after injury using immunohistochemistry.

In the spinal cords of the control animals (medium-1w-isp), modest MMP-2 immunoreactivity was detected in the cavity wall of the spinal cords at the level of the epicenter, gradually decreasing toward both ends of the cavity (Supplementary Fig. S4A,A′; see online supplementary material at www.liebertpub.com). More increased MMP-2 expression was found in the NE4C-immed-iv and NE4C-1w-iv groups mainly locating to the epicenter, but in contrast with the medium-1w-isp group, MMP-2 displayed more intense expression in the host tissue (Supplementary Fig. S4B,B′,C,C′). Strong MMP-2 immunoreaction was detected in the grafted cells and in the cavity wall of NE4C-1w-isp rats (Supplementary Fig. S4D,D′,E,E′,E″). The MMP-2 expression was highest in the middle of the graft and appeared to be significantly weaker toward its cranial and caudal ends.

Factors produced by grafted stem cells induce functional recovery in the intraspinally grafted animals

In the case of intraspinal grafting, the transplanted cells are apposed to the wall of the cavity. The fact that only limited numbers of graft-derived cells settled in the wall of the cavity suggested that there is a paracrine secretory mechanism acting on the host spinal cord. To determine the factors secreted by the grafted cells, we analyzed the expression of 10 factors (IL-1-alpha, IL-6, IL-10, TNF-alpha, MIP-1-alpha, NT-4/5, BDNF, GDNF, VEGF, PDGF-A), thought to exert beneficial effects on the damaged cord.

Four of the 10 factors were found to be expressed in the graft (GDNF, IL-6, IL-10 and MIP-1a) (Fig. 5). The GDNF showed strong expression patterns both in the host cord and in the graft (Fig. 5A,A′,A″). Strong IL-6 expression was confined to the grafted cells accompanied by weaker staining in the host spinal cord (Fig. 5B, B′, B″). The IL-10 and MIP-1a expressions showed similar distribution patterns to that of GDNF, but the expression of these two factors within the host cord was restricted to the tissue located ventral to the cavity (Fig. 5C,C′,C″,D,D′,D″).

Interestingly, the control group animals (medium-1w-isp) that did not receive any graft showed no expression of the various factors (Fig. 5E,F,G,H). Comparison of immunoreactivity of all four factors across the control (medium-1w-isp) and grafted

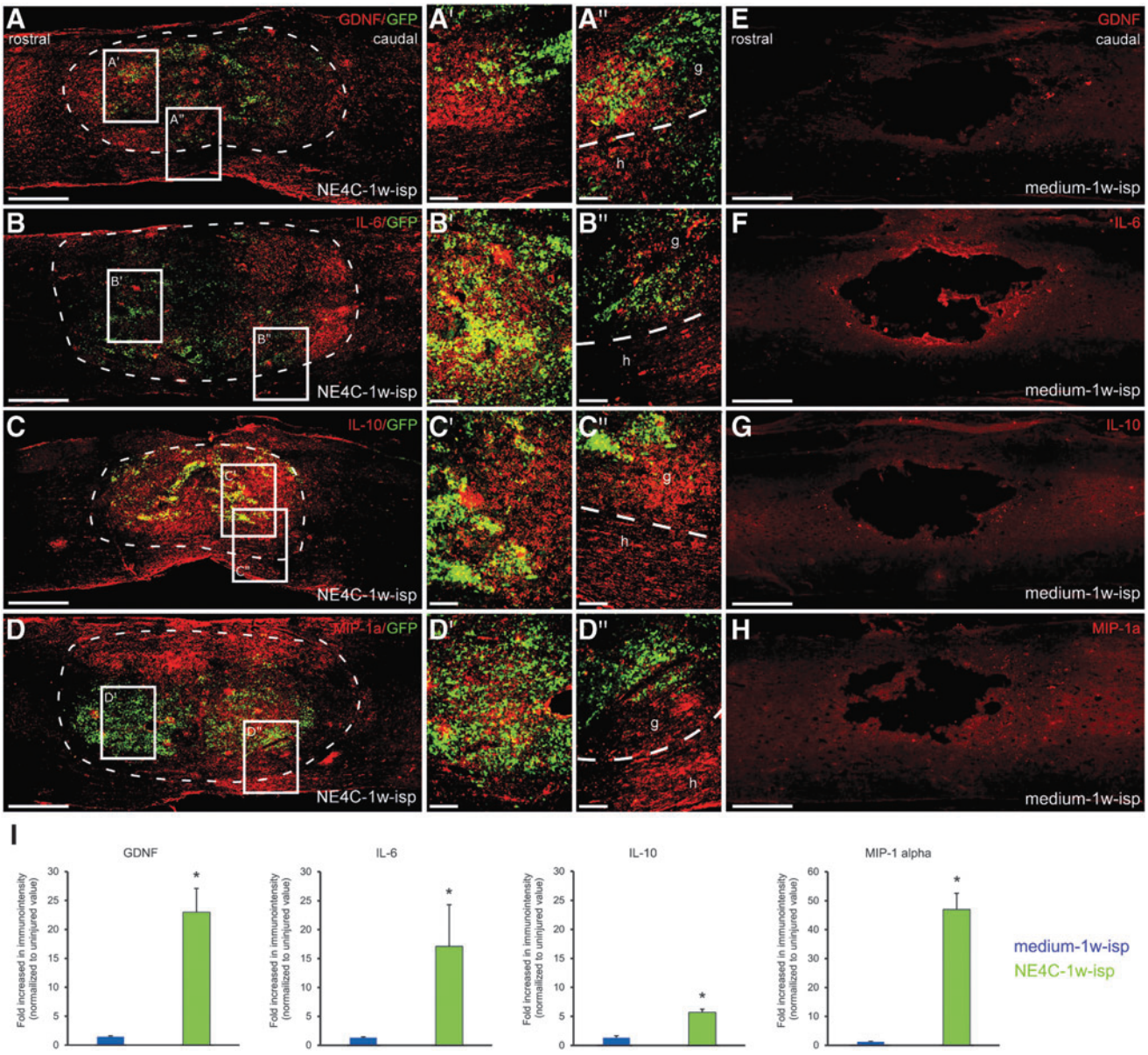

FIG. 5. Expression of the various factors produced by the intraspinally grafted NE-GFP-4C stem cells and host spinal cord tissue one week after grafting. (**A–D**): The graft and the host tissues express glial cell derived neurotrophic factor (GDNF), interleukin (IL-)6, IL-10, and macrophage inflammatory protein (MIP)-1a. A′–D′ show the strong expression pattern of these factors within the graft (boxed areas taken from the graft region). In contrast, A″–D″ show the interface region between the graft (g) and the host (h) tissues with varying extent of expression intensity in the host (boxed areas taken from the graft-host interface). (**E–H**) None of these factors was found to be expressed in the spinal cords of control animals (medium-1w-isp). (**I**) Quantification of all four factors revealed an increased level of GDNF, IL6, IL-10, and MIP-1a immunoreactivity in intraspinally grafted group (NE4C-1w-isp) compared with controls (medium-1w-isp). Dashed line indicates the graft-host border. Data are expressed as mean ± standard error of the mean. *, significant difference between NE4C-1w-isp group with the control group (medium-1w-isp). Scale bars: A–H: 500 μm, A′–D′, A″–D″: 100 μm. Color image is available online.

(NE4C-1w-isp) experimental spinal cords revealed a robust increase in GDNF, IL-6, IL-10, and MIP-1 alpha expression in the host tissue of grafted group (Fig. 5I).

To test whether these three cytokines and GDNF are indeed responsible for inducing the rescue and regeneration of the host neurons, we used osmotic minipumps to infuse the mixture of function blocking mouse-specific antibodies produced against all four factors to the grafts in a separate set of animals (NE4C-isp-blocking). Motor recovery of the hindlimbs was evaluated, and the results were compared with those of the control (medium-1w-isp) and intraspinally treated group (NE4C-1w-isp; Fig. 6). Blocking of function of the proteins produced by the grafted cells resulted in similarly poor recovery as found in control animals (Fig. 6A). Despite the use of neutralizing antibodies, the grafted stem cells survived and differentiated to the same extent as the stem cells within the intraspinally grafted animals (Fig. 6B,B′,C,C′,D,D′).

To test whether active immunoglobulins used in these experiments do not have a neutralizing effect on the grafted stem cells, osmotic

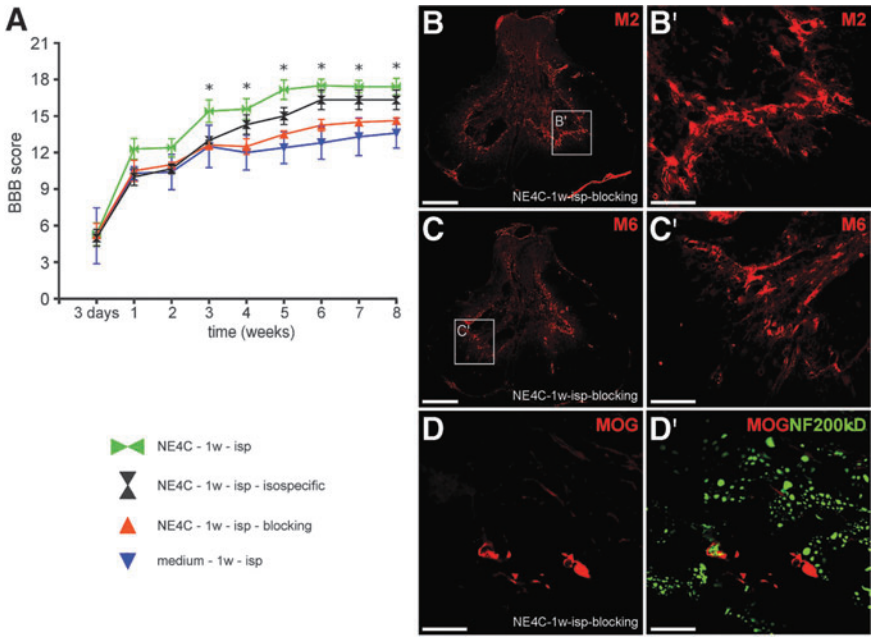

FIG. 6. Functional blocking of the factors produced by the stem cells with neutralizing antibodies abolishes the motor recovery in grafted animals. (**A**): Open field locomotor test (Basso, Beattie, Bresnahan) shows that grafted animals (NE4C-isp-blocking) treated with neutralizing antibodies against the four secretome factors produce as little recovery as control rats (medium-1w-isp). Animals treated with isospecific immune globulin G (IgGs) (NE4C-1w-isp-isospecific) showed considerable improvement. The non-significant difference between NE4C-1w-isp and NE4C-1w-isp-isospecific groups is likely because of the effect of the implanted osmotic pump and tube. (**B–D**): Grafted animals treated with neutralizing antibodies also displayed surviving stem cell-derived astroglial cells (B, B′), neurons (C,C′), and oligodendrocytes in close relationship with NF-200 positive axons (D,D′). The presence of stem cell-derived cells may be responsible for the non-significant difference between NE4C-isp-blocking and medium-1w-isp groups. Data are expressed as mean ± standard error of the mean. *, significant difference between the intraspinally grafted animals with the control ones. B,C: 500 μm, B′,C′: 100 μm, D,D′: 50 μm. Color image is available online.

pumps filled with a mixture of isotype-specific IgGs were used to deliver these IgGs to the site of grafting (NE4C-isp-isospecific). No significant difference relative to the intraspinally grafted animals was found (Fig. 6A).

Expression of IL-10 in intravenous groups

In the intravenously treated animals (NE4C-immed-iv, NE4C-1w-iv), only IL-10 was found to be expressed at immunohistochemically detectable levels. Expression of IL-10 was confined mainly to the internal margin of the cavity and to its wall composed of host tissue (Supplementary Fig. S5A,A′,B,B′, respectively; see online supplementary material at www.liebertpub.com). To determine the source of IL-10, we performed immunohistochemical double labeling. Astrocytes were found to express IL-10 around the cavity (Fig. S5C). In the internal marginal zone of the cavity, round GSA-B4-positive macrophages displayed IL-10 immunoreactivity (Fig. S5D).

Discussion

Grafted stem cells induce tissue sparing, axonal sparing/regeneration, and functional recovery

Both intraspinal and intravenous application of NE-GFP-4C cells promoted tissue sparing in the injured cords. The significant amount of spared white matter made it possible to maintain the temporarily disrupted connections between the intact regions above and below the injury site. The considerable white matter sparing is supported by the fact that the lumbar cords of grafted animals displayed limited sprouting of 5-HT fibers compared with control cords. The limited sprouting may indicate the presence of a higher number of supplying 5-HT fibers as supported by our retrograde labeling studies.

On the other hand, it became evident from the anterograde labeling studies of the CST tract that, apart from tract sparing, a significant number of descending CST fibers was able to regenerate along a new pathway, and this regeneration was supported by the permissive environment around the lesion. Although not investigated, it can be argued that similar to the CST tract, other minor and major tracts may have regenerated, too. The rescue of gray matter and short propriospinal tracts may also have contributed to the functional restoration of the damaged cords.[45,46] These considerable morphological improvements observed in the grafted cords led to the significant functional recovery.

In our study, a higher number of retrograde labeled brainstem neurons could be detected in stem cells grafted groups compared with controls. Regeneration of brainstem neurons is essential for locomotor functional recovery in the rat after SCI.[47,48] Thus, regeneration/sparing of these neurons has the potential to improve functional recovery if they reach or retain their connection with the targets distal to the lesion.

The spinal serotonergic pathway showed axonal sprouting, which may play a pivotal role in neuromodulation and locomotion.[34,35] Previous studies have demonstrated that increased 5-HT fiber density in the injured spinal cord contributes to improved functional recovery.[49,50] In contrast, we found that increased

density of sprouting serotonergic fibers below the lesion was not associated with significantly improved recovery of locomotion. It could be argued that serotonergic fiber preservation in the grafted animals did induce less sprouting than that observed in control animals, where the remaining serotonergic axons likely produced considerably sprouting.

These data further suggest that an aligned and target-oriented supraspinal innervation of spinal cord regions distal to the injury may act more effectively than abundant and uncontrolled sprouting of these fibers. These data accord with the finding that in the intraspinally grafted animals, higher numbers of raphe neurons were retrograde labeled from segments distal to the lesion, indicating a preserved aligned 5-HT fiber tract structure with lower 5-HT densities in these segments. This is contrasted by the fewer retrograde labeled raphe cells associated with higher 5-HT fiber densities in the other experimental groups, suggesting considerable sprouting derived from the fewer surviving axons.

Microenvironment in the grafted cords is permissive for regenerating axons

In this study, we have demonstrated that NE-GFP-4C grafting induced significantly lower astrocyte/microglia reaction than found in the control spinal cords. This resulted in lower amounts of CS-56 and ephrin-B2 in the microenvironment of the lesion, and these favorable changes rendered the glial scar permissive for axonal regeneration.[51,52] Moreover, the matrix metalloproteinase isozyme MMP-2 reportedly shows an inverse expression pattern with the amount of the developing glial scar tissue after SCI. Higher levels of MMP-2 densities may suggest the development of less dense glial scar in the injured cord by regulating the formation of a glial scar and white matter sparing and/or axonal plasticity.[42,53] In the spinal cords of the grafted animals, significantly higher densities of MMP-2 were observed within the graft and in the surrounding host tissue than in control cords.

It can be argued that these above outlined changes (astrocyte/microglia downregulation along with associated low densities of CS-56 and ephrin-B2 and upregulation of MMP-2 production) all induced an altered lesion microenvironment that promoted the regeneration of injured axons.

It was surprising to see that human fibrin treatment alone did not improve the functional outcome or gliosis of the lesion site. Moreover, animals treated with NE-GFP-4C cells embedded in human fibrin had more impaired functional outcome and more extensive gliosis than the control animals, including its own control group. This phenomenon can be explained on the basis of recent findings that prove the rather negative effect of mammalian fibrin matrices on the injured spinal cord in contrast to non-mammalian (salmon) fibrin.[54] It can also be argued that the disintegrating mammalian fibrin matrix may have induced a consequent degeneration/death of the grafted stem cells leading to tertiary damage within the contused cords replacing the regenerative effects of the stem cells.

Factors contributing to functional recovery

Our results suggest that the grafted stem cells may contribute to the improved functional recovery after contusion injury by a dual mechanism. It appears evident that the grafted cells produce a set of cytokines (IL-6, IL-10, and MIP-1a) and GDNF. Functional blocking of these factors produced by the grafted cells in the intraspinal grafting group have provided evidence that they play a major role in the functional recovery process compared with the effect of stem cell derivatives that remained in the wall of the lesion cavity.

It could be argued that the non-significant difference found in the functional improvement of the animals that received functional blocking treatment compared with their controls may be because of the presence of various stem cell derivatives (neurons, astrocytes, and myelinating oligodendrocytes) around the lesion cavity. The low number of these cells suggests that other minor effects may have contributed to this difference in the functional outcome.

These findings support the hypothesis that in the case of intraspinal grafting of NE-GFP-4C stem cells, the mechanism of action is based on the major paracrine immunomodulatory and neurotrophic effect and on a minor cellular replacement mechanism. The fact that in the intravenous grafting groups only IL-10 was expressed around the lesion and no stem cell derivatives were found at the end of the survival period explains the somewhat limited efficacy of this grafting method.

The intravenous application of NE-GFP-4C cells was able to reduce the microglia/macrophage reactions in the affected spinal cord segments. These results suggest that intravenously applied NE-GFP-4C cells may exert their primary effects outside the spinal cord perhaps by altering the immune-mediated secondary pathological events after SCI. This phenomenon requires further studies to elucidate the mechanism.

Our findings have shown clearly that the paracrine effect was exerted by the undifferentiated stem cells only soon after grafting. As reported by our laboratory earlier, NE-GFP-4C cells do not produce any of these factors in culture.[26] Accordingly, the grafted cells start factor production after a short period after grafting, and this suggests the presence of a strong communicative interaction between the injured host tissue and the grafted cells.

The efficacy of GDNF to enhance axonal growth through and beyond the injury site has been proven by several studies.[25,55,56] Moreover, local spinal neurons and glial cells can also be rescued by GDNF treatment during the acute phase of the injury,[57] and neosynaptogenesis has reportedly been enhanced as well.[58] The IL-6 proved to be neuroprotective against excitotoxicity-induced cell death in the CNS via distinct pathways.[59,60] *In vitro* administration of IL-6 enhances neurite outgrowth of neurons accompanied by increased expression of growth associated genes.[61]

The IL-10 is a strong anti-inflammatory cytokine of the immune system and has a neuroprotective effect in the CNS, too. Administration of IL-10 after traumatic or excitotoxic SCI promoted survival of the injured neurons and improved the motor recovery by acting on the injured neurons.[62] The exact role of MIP-1a is not fully understood in the injured CNS, but our laboratory showed that it has a role in the motoneuron survival after SCI.[63]

Conclusion

We can state that grafted NE-GFP-4C neuroectodermal stem cells induce robust regeneration and neuroprotection in the injured spinal cord. This effect is because of paracrine secretion mechanism of the transplanted cells producing GDNF, MIP-1a, IL-6, and IL-10. Only a minor, non-significant improvement may be induced by stem cell-derived neurons and glia settled in the wall of the contusion cavity. The secreted factors appeared to have rendered the microenvironment axonal growth-permissive and prevented the death of damaged neurons and glial cells otherwise destined to die.

Acknowledgments

We thank the generous financial support of the OTKA/NKFIH (National Scientific Foundation, Hungary, Grant No.: KLINO-117031) and the Lorenz Böhler Foundation, Austria.

Author Disclosure Statement

No competing financial interests exist.

Supplementary Material

Supplementary Figure S1
Supplementary Figure S2
Supplementary Figure S3
Supplementary Figure S4
Supplementary Figure S5

References

1. Fouad, K., Klusman, I., and Schwab, M.E. (2004). Regenerating corticospinal fibers in the Marmoset (Callitrix jacchus) after spinal cord lesion and treatment with the anti-Nogo-A antibody IN-1. Eur. J. Neurosci. 20, 2479–2482.
2. Garbossa, D., Boido, M., Fontanella, M., Fronda, C., Ducati, A., and Vercelli, A. (2012). Recent therapeutic strategies for spinal cord injury treatment: possible role of stem cells. Neurosurg. Rev. 35, 293–311.
3. Bethea, J.R., Nagashima, H., Acosta, M.C., Briceno, C., Gomez, F., Marcillo, A.E., Loor, K., Green, J., and Dietrich, W.D. (1999). Systemically administered interleukin-10 reduces tumor necrosis factor-alpha production and significantly improves functional recovery following traumatic spinal cord injury in rats. J. Neurotrauma 16, 851–863.
4. Kamencic, H., Griebel, R.W., Lyon, A.W., Paterson, P.G., and Juurlink, B.H. (2001). Promoting glutathione synthesis after spinal cord trauma decreases secondary damage and promotes retention of function. FASEB J. 15, 243–250.
5. Takami, T., Oudega, M., Bethea, J.R., Wood, P.M., Kleitman, N., and Bunge, M.B. (2002). Methylprednisolone and interleukin-10 reduce gray matter damage in the contused Fischer rat thoracic spinal cord but do not improve functional outcome. J. Neurotrauma 19, 653–666.
6. Beattie, M.S. (2004). Inflammation and apoptosis: linked therapeutic targets in spinal cord injury. Trends Mol. Med. 10, 580–583.
7. Aslan, A., Cemek, M., Buyukokuroglu, M.E., Altunbas, K., Bas, O., Yurumez, Y., and Cosar M. (2009). Dantrolene can reduce secondary damage after spinal cord injury. Eur. Spine J. 18, 1442–1451.
8. Haque, A., Capone, M., Matzelle, D., Cox, A., and Banik, N.L. (2017). Targeting enolase in reducing secondary damage in acute spinal cord injury in rats. Neurochem. Res. 42(, 2777–2787.
9. Figueroa, J.D., Benton, R.L., Velazquez, I., Torrado, A.I., Ortiz, C.M., Hernandez, C.M., Diaz, J.J., Magnuson, D.S., Whittemore, S.R., and Miranda, J.D. (2006). Inhibition of EphA7 up-regulation after spinal cord injury reduces apoptosis and promotes locomotor recovery. J. Neurosci. Res. 84, 1438–1451.
10. Goldshmit, Y., Spanevello, M.D., Tajouri, S., Li L., Rogers, F., Pearse, M., Galea, M., Bartlett, P.F., Boyd, A.W., and Turnley, A.M. (2011). EphA4 blockers promote axonal regeneration and functional recovery following spinal cord injury in mice. PLoS One. 6, e24636.
11. Ren, Z., Chen, X., Yang, J., Kress, B.T., Tong, J., Liu, H., Takano, T., Zhao, Y., and Nedergaard, M. (2013). Improved axonal regeneration after spinal cord injury in mice with conditional deletion of ephrin B2 under the GFAP promoter. Neuroscience 241, 89–99.
12. Qu, Y., Zhao, J., Wang, Y., and Gao, Z. (2014). Silencing ephrinB3 improves functional recovery following spinal cord injury. Mol. Med. Rep. 9, 1761–1766.
13. Kubo, T., Hata, K., Yamaguchi, A., and Yamashita, T. (2007). Rho-ROCK inhibitors as emerging strategies to promote nerve regeneration. Curr. Pharm. Des. 13, 2493–2499.
14. Wu, B.Q., Bi, Z.G., and Qi, Q. (2013). Inactivation of the Rho-ROCK signaling pathway to promote neurologic recovery after spinal cord injuries in rats. Chin. Med. J. (Engl) 126, 3723–3727.
15. Wang, J.W., Yang, J.F., Ma, Y., Hua, Z., Guo, Y., Gu, X.L., and Zhang, Y.F. (2015). Nogo-A expression dynamically varies after spinal cord injury. Neural. Regen. Res. 10, 225–229.
16. Zuo, J., Hernandez, Y.J., and Muir, D. (1998). Chondroitin sulfate proteoglycan with neurite-inhibiting activity is up-regulated following peripheral nerve injury. J. Neurobiol. 34, 41–54.
17. McKillop, W.M., Dragan, M., Schedl, A., and Brown, A. (2013). Conditional Sox9 ablation reduces chondroitin sulfate proteoglycan levels and improves motor function following spinal cord injury. Glia 61, 164–177.
18. Schwartz, G., and Fehlings. M.G. (2002). Secondary injury mechanisms of spinal cord trauma: a novel therapeutic approach for the management of secondary pathophysiology with the sodium channel blocker riluzole. Prog. Brain Res. 137, 177–190.
19. Pintér, S., Gloviczki, B., Szabó, A., Márton, G., and Nógrádi, A. (2010). Increased survival and reinnervation of cervical motoneurons by riluzole after avulsion of the C7 ventral root. J. Neurotrauma 27, 2273–2282.
20. Salewski, R.P., Mitchell, R.A., Li, L., Shen, C., Milekovskaia, M., Nagy, A., and Fehlings, M.G. (2015). Transplantation of induced pluripotent stem cell-derived neural stem cells mediate functional recovery following thoracic spinal cord injury through remyelination of axons. Stem Cells Transl. Med. 4, 743–754.
21. Stamegna, J.C., Sadelli, K., Escoffier, G., Girard, S.D., Veron, A.D., Bonnet, A., Khrestchatisky, M., Gauthier, P., and Roman, F.S. (2018). Grafts of olfactory stem cells restore breathing and motor functions after rat spinal cord injury. J. Neurotrauma 35, 1765–1780.
22. Riemann, L., Younsi ,A., Scherer, M., Zheng, G., Skutella, T., Unterberg, A.W., and Zweckberger K. (2018). Transplantation of neural precursor cells attenuates chronic immune environment in cervical spinal cord injury. Front. Neurol. 9, 428.
23. Levi, A.D., Anderson, K.D., Okonkwo, D.O., Park, P., Bryce, T.N., Kurpad, S.N., Aarabi, B., Hsieh, J., and Gant, K. (2019). Clinical outcomes from a multi-center study of human neural stem cell transplantation in chronic cervical spinal cord injury. J. Neurotrauma 36, 891–902.
24. Schlett, K., Herberth, B., and Madarász, E. (1997). In vitro pattern formation during neurogenesis in neuroectodermal progenitor cells immortalized by p53-deficiency. Int. J. Dev. Neurosci. 15, 795–804.
25. Pajenda, G., Pajer, K., Márton, G., Hegyi, P., Redl, H., and Nógrádi, A. (2013). Rescue of injured motoneurones by grafted neuroectodermal stem cells: effect of the location of graft. Restor. Neurol. Neurosci. 31, 263–274.
26. Pajer, K., Feichtinger, G.A., Márton, G., Sabitzer, S., Klein, D., Redl, H., and Nógrádi, A. (2014). Cytokine signaling by grafted neuroectodermal stem cells rescues motoneurons destined to die. Exp. Neurol. 261, 180-189.
27. Péron, S., Droguerre, M., Debarbieux, F., Ballout, N., Benoit-Marand, M., Francheteau, M., Brot, S., Rougon, G., Jaber, M., and Gaillard, A. (2017). A delay between motor cortex lesions and neuronal transplantation enhances graft Integration and improves repair and recovery. J. Neurosci. 37, 1820–1834.
28. Hill, C.E., Beattie, M.S., and Bresnahan, J.C. (2001). Degeneration and sprouting of identified descending supraspinal axons after contusive spinal cord injury in the rat. Exp. Neurol. 171, 153–169.
29. Bunge, M.B. (2002). Bridging the transected or contused adult rat spinal cord with Schwann cell and olfactory ensheathing glia transplants. Prog. Brain Res. 137, 275–282.
30. Karimi-Abdolrezaee, S., Eftekharpour, E., Wang, J., Schut, D., and Fehlings, M.G. (2010). Synergistic effects of transplanted adult neural stem/progenitor cells, chondroitinase, and growth factors promote functional repair and plasticity of the chronically injured spinal cord. J. Neurosci. 30, 1657–1676.
31. Basso, D.M., Beattie, M.S., and Bresnahan, J.C. (1995). A sensitive and reliable locomotor rating scale for open field testing in rats. J. Neurotrauma 12, 1–21.
32. Hamers, F.P., Lankhorst, A.J., van Laar, T.J., Veldhuis, W.B., and Gispen, W.H. (2001). Automated quantitative gait analysis during overground locomotion in the rat: its application to spinal cord contusion and transection injuries. J. Neurotrauma 18, 187–201.
33. Deumens, R., Koopmans, G.C., Honig, W.M., Maquet ,V., Jérôme, R., Steinbusch, H.W., and Joosten, E.A. (2006). Chronically injured corticospinal axons do not cross large spinal lesion gaps after a multifactorial transplantation strategy using olfactory ensheathing cell/olfactory nerve fibroblast-biomatrix bridges. J. Neurosci. Res. 83, 811–820.
34. Schmidt, B.J. and Jordan, L.M. (2000). The role of serotonin in reflex modulation and locomotor rhythm production in the mammalian spinal cord. Brain Res. Bull. 53, 689–710.
35. Sławińska, U., Miazga, K., Cabaj, A.M., Leszczyńska, A.N., Majczyński, H., Nagy, J.I., and Jordan, L.M. (2013). Grafting of fetal brainstem 5-HT neurons into the sublesional spinal cord of paraplegic rats restores coordinated hindlimb locomotion. Exp. Neurol. 247, 572–581.

36. Leszczyńska, A.N., Majczyński, H., Wilczyński, G.M., Sławińska, U., and Cabaj, A.M. (2015). Thoracic hemisection in rats results in initial recovery followed by a late decrement in locomotor movements, with changes in coordination correlated with serotonergic innervation of the ventral horn. PLoS One 10, e0143602.
37. Willson, C.A., Irizarry-Ramírez, M., Gaskins, H.E., Cruz-Orengo, L., Figueroa, J.D., Whittemore, S.R., and Miranda, J.D. (2002). Upregulation of EphA receptor expression in the injured adult rat spinal cord. Cell Transplant. 11, 229–239.
38. Duffy, P., Wang, X., Siegel, C.S., Tu, N., Henkemeyer, M., Cafferty, W.B., and Strittmatter, S.M. (2012). Myelin-derived ephrinB3 restricts axonal regeneration and recovery after adult CNS injury. Proc. Natl. Acad. Sci. U. S. A. 109, 5063–5068.
39. Wahl, S., Barth, H., Ciossek, T., Aktories, K., and Mueller, B.K. (2000). Ephrin-A5 induces collapse of growth cones by activating Rho and Rho kinase. J. Cell Biol. 149, 263–270.
40. Fabes, J., Anderson, P., Yáñez-Muñoz, R.J., Thrasher, A., Brennan, C., and Bolsover, S. (2006). Accumulation of the inhibitory receptor EphA4 may prevent regeneration of corticospinal tract axons following lesion. Eur. J. Neurosci. 23, 1721–1730.
41. Pizzi, M.A. and Crowe, M.J. (2007). Matrix metalloproteinases and proteoglycans in axonal regeneration. Exp. Neurol. 204, 496–511.
42. Hsu, J.Y., McKeon, R., Goussev, S., Werb, Z., Lee, J.U., Trivedi, A., and Noble-Haeusslein, L.J. (2006). Matrix metalloproteinase-2 facilitates wound healing events that promote functional recovery after spinal cord injury. J. Neurosci. 26, 9841–9850.
43. Zhang, H., Chang, M., Hansen, C.N., Basso, D.M., and Noble-Haeusslein, L.J. (2011). Role of matrix metalloproteinases and therapeutic benefits of their inhibition in spinal cord injury. Neurotherapeutics 8, 206–220.
44. Trivedi, A., Zhang, H., Ekeledo, A., Lee, S., Werb, Z., Plant, G.W., and Noble-Haeusslein, L.J. (2016). Deficiency in matrix metalloproteinase-2 results in long-term vascular instability and regression in the injured mouse spinal cord. Exp. Neurol. 284, 50–62.
45. Conta, A.C. and Stelzner, D.J. (2004). Differential vulnerability of propriospinal tract neurons to spinal cord contusion injury. J. Comp. Neurol. 479, 347–359.
46. Vavrek, R., Girgis, J., Tetzlaff, W., Hiebert, G.W., and Fouad, K. (2006). BDNF promotes connections of corticospinal neurons onto spared descending interneurons in spinal cord injured rats. Brain 129, 1534–1545.
47. Basso, D.M., Beattie, M.S., and Bresnahan, J.C. (2002). Descending systems contributing to locomotor recovery after mild or moderate spinal cord injury in rats: experimental evidence and a review of literature. Restor. Neurol. Neurosci. 20, 189–218.
48. Ghosh, M. and Pearse, D.D. (2015). The role of the serotonergic system in locomotor recovery after spinal cord injury. Front. Neural Circuits 8, 151.
49. Holmes, G.M., Van Meter, M.J., Beattie, M.S., and Bresnahan, J.C. (2005). Serotonergic fiber sprouting to external anal sphincter motoneurons after spinal cord contusion. Exp. Neurol. 193, 29–42.
50. Li, S. and Strittmatter, S.M. (2003). Delayed systemic Nogo-66 receptor antagonist promotes recovery from spinal cord injury. J. Neurosci. 23, 4219–4227.
51. Morgenstern, D.A., Asher, R.A., and Fawcett, J.W. (2002). Chondroitin sulphate proteoglycans in the CNS injury response. Prog. Brain Res. 137, 313–332.
52. Dyck, S.M. and Karimi-Abdolrezaee, S. (2015). Chondroitin sulfate proteoglycans: key modulators in the developing and pathologic central nervous system. Exp. Neurol. 269, 169–187.
53. Veeravalli, K.K., Dasari, V.R., Tsung, A.J., Dinh, D.H., Gujrati, M., Fassett, D., and Rao, J.S. (2009). Human umbilical cord blood stem cells upregulate matrix metalloproteinase-2 in rats after spinal cord injury. Neurobiol. Dis. 36, 200–212.
54. Sharp, K.G., Dickson, A.R., Marchenko, S.A., Yee, K.M., Emery, P.N., Laidmåe, I., Uibo, R., Sawyer, E.S., Steward, O., and Flanagan, L.A. (2012). Salmon fibrin treatment of spinal cord injury promotes functional recovery and density of serotonergic innervation. Exp. Neurol. 235, 345–356.
55. Iannotti, C., Li, H., Yan, P., Lu, X., Wirthlin, L., and Xu, X.M. (2003). Glial cell line-derived neurotrophic factor-enriched bridging transplants promote propriospinal axonal regeneration and enhance myelination after spinal cord injury. Exp. Neurol. 183, 379–393.
56. Sivak, W.N., White, J.D., Bliley, J.M., Tien, L.W., Liao, H.T., Kaplan, D.L., and Marra, K.G. (2017). Delivery of chondroitinase ABC and glial cell line-derived neurotrophic factor from silk fibroin conduits enhances peripheral nerve regeneration. J. Tissue Eng. Regen. Med. 11, 733–742.
57. Oppenheim, R.W., Houenou, L.J., Johnson, J.E., Lin, L.F., Li, L., Lo, A.C., Newsome, A.L., Prevette, D.M., and Wang, S. (1995). Developing motor neurons rescued from programmed and axotomy-induced cell death by GDNF. Nature 373, 344–346.
58. Ledda, F., Paratcha, G., Sandoval-Guzmán, T., and Ibáñez, C.F. (2007). GDNF and GFRalpha1 promote formation of neuronal synapses by ligand-induced cell adhesion. Nat. Neurosci. 10, 293–300.
59. Carlson, N.G., Wieggel, W.A., Chen, J., Bacchi, A., Rogers, S.W., and Gahring, L.C. (1999). Inflammatory cytokines IL-1 alpha, IL-1 beta, IL-6, and TNF-alpha impart neuroprotection to an excitotoxin through distinct pathways. J. Immunol. 163, 3963–3968.
60. Leibinger, M., Müller, A., Gobrecht, P., Diekmann, H., Andreadaki, A., and Fischer, D. (2013). Interleukin-6 contributes to CNS axon regeneration upon inflammatory stimulation. Cell Death Dis. 4, e609.
61. Yang, P., Wen, H., Ou, S., Cui, J., and Fan, D. (2012). IL-6 promotes regeneration and functional recovery after cortical spinal tract injury by reactivating intrinsic growth program of neurons and enhancing synapse formation. Exp. Neurol. 236, 19–27.
62. Zhou, Z., Peng, X., Insolera, R., Fink, D.J., and Mata, M. (2009). Interleukin-10 provides direct trophic support to neurons. J. Neurochem. 110, 1617–1627.
63. Pajer, K., Nemes, C., Berzsenyi, S., Kovács, K.A., Pirity, M.K., Pajenda, G., Nógrádi, A., and Dinnyés, A. (2015). Grafted murine induced pluripotent stem cells prevent death of injured rat motoneurons otherwise destined to die. Exp. Neurol. 269, 188–201.

Address correspondence to:
Antal Nógrádi, MD, PhD, DSc
Department of Anatomy, Histology, and Embryology
University of Szeged
Kossuth Lajos sgt. 40
H-6724, Szeged
Hungary

E-mail: nogradi.antal@med.u-szeged.hu